

Efficient Generalized Cross-Validation with Applications to Parametric Image Restoration and Resolution Enhancement

Nhat Nguyen, Peyman Milanfar, *Senior Member, IEEE*, and Gene Golub

Abstract—In many image restoration/resolution enhancement applications, the blurring process, i.e., point spread function (PSF) of the imaging system, is not known or is known only to within a set of parameters. We estimate these PSF parameters for this ill-posed class of inverse problem from raw data, along with the regularization parameters required to stabilize the solution, using the generalized cross-validation method (GCV). We propose efficient approximation techniques based on the Lanczos algorithm and Gauss quadrature theory, reducing the computational complexity of the GCV. Data-driven PSF and regularization parameter estimation experiments with synthetic and real image sequences are presented to demonstrate the effectiveness and robustness of our method.

Index Terms—Blind restoration, blur identification, generalized cross-validation, quadrature rules, superresolution.

I. INTRODUCTION

IMAGE resolution enhancement¹ refers to image processing algorithms which produce high quality, high-resolution (HR) images from a set of low-quality, low-resolution (LR) images. While there is always a demand for better quality images, the level of image detail is crucial in the performance of several computer vision algorithms. Target recognition, detection and identification systems are some of the military applications which require highest quality achievable images. License plate readers, surveillance monitors, and medical imaging applications are examples of civilian applications with the same requirement. In many visual applications, both civilian and military, the imaging sensors have poor resolution outputs. When resolution can not be improved by replacing sensors, either because of cost or hardware physical limits, we can resort to video resolution enhancement algorithms. Even

when superior equipment is available, resolution enhancement algorithms can provide an inexpensive alternative.

A related problem, image restoration is a well-known area of research with many established algorithms. Image restoration produces an estimate of the original image given a degraded image *at the same resolution scale*. Not surprisingly, restoration and resolution enhancement are closely related problems. In fact, image restoration is simply a special case of resolution enhancement.

In this paper, we are mainly interested in robust techniques for solving restoration and resolution enhancement in imperfectly known imaging conditions. We consider when the blurring process is known only to within a set of parameters, and the noise process variance's unknown. We propose efficient techniques for parametric blur identification and regularization based on generalized cross-validation and Gauss quadrature theory.

The rest of this paper is organized as follows. In Section II, we outline the problem description and model for resolution enhancement. Image restoration is a special case of resolution enhancement, and Section III shows the relationship between them. Techniques for PSF and regularization parameter estimation proposed in this paper can be applied equally well to resolution enhancement or restoration. Sections IV and V describe the blur identification problem and our approach using the generalized cross-validation (GCV) method in detail. In Section VI, we present our method for approximating the GCV criterion value accurately and efficiently, based on quadrature rules and the Lanczos algorithm. Blur estimation and resolution enhancement results are shown in Section VII.

II. PROBLEM DESCRIPTION

In this section, we describe a straightforward and efficient model for resolution enhancement which will serve as the foundation for the development of algorithms for the rest of the paper. We assume consistent lighting conditions, negligible optical distortions, that objects observed are acquired under orthographic projections, and that individual scene motions can be modeled, or approximated, as affine transformations. While these simplifications result in some loss of generality, the model will be adequate for the majority of resolution enhancement imaging applications.

The problem can be stated as follows.

Given a set of degraded LR frames $\{\mathbf{f}_k\}_{k=1,\dots,p}$ each $M \times N$ pixels in dimension under the conditions above,

Manuscript received February 29, 2000; revised April 3, 2001. This work was supported in part by the National Science Foundation under Grants CCR-9505393 and CCR-9984246. The associate editor coordinating the review of this manuscript and approving it for publication was Prof. Timothy J. Schulz.

N. Nguyen and G. Golub are with the Scientific Computing and Computational Mathematics Program, Stanford University, Stanford, CA 94305-9025 USA (e-mail: nguyen@sccm.stanford.edu; golub@sccm.stanford.edu).

P. Milanfar is with the Department of Electrical Engineering, University of California, Santa Cruz, CA 95064 USA (e-mail: milanfar@ee.ucsc.edu).

Publisher Item Identifier S 1057-7149(01)06040-7.

¹A related class of algorithms is the superresolution algorithms [18]. Traditionally, the term *superresolution* has been used to mean algorithms capable of extracting bandwidth frequencies beyond diffraction limit of the optical system. These algorithms mainly operate on a single image. More recently, *superresolution* has also been used for algorithms which obtain higher spatial resolution by interpolating subpixel information from multiple images. To avoid ambiguity, we use *resolution enhancement* in this paper.

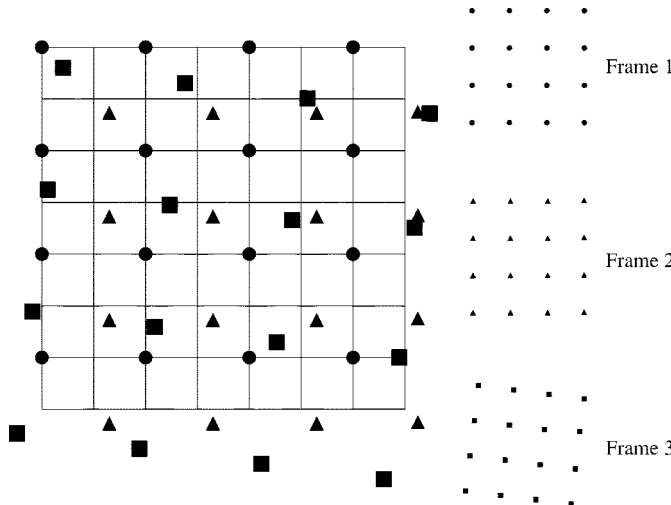


Fig. 1. Low-resolution data on a high-resolution grid.

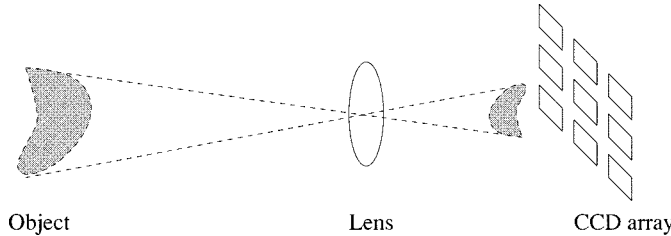


Fig. 2. CCD camera model.

and a desired enhancement factor r , reconstruct an enhanced/restored HR image with dimensions $rM \times rN$.

Fig. 1 illustrates the problem setup. The figure shows three 4×4 pixel LR frames on an 8×8 HR grid. Each symbol (square, circle, triangle) indicates the sampling points of a frame with respect to the HR grid. We pick an arbitrary frame as a reference frame; in this case, the frame marked by the circular symbols. The sampling grid for the triangular frame is a simple translation of the reference frame grid. The difference between the sampling grid for the square frame and the reference frame grid includes translational, rotational, and magnification (zoom) components. The goal of resolution enhancement is to interpolate and restore values at the HR grid points.

In order to solve for the unknown HR values, we first model the forward process, which takes the ideal HR image to a degraded LR frame. Many imaging devices today utilize charged-coupled devices (CCD) which are arrays of light detectors. A detector determines pixel intensity values depending upon the amount of light detected from its respective area in the scene. Resolution of images produced by the camera is proportional to the density of the detector array. Fig. 2 shows a simplistic model of a CCD camera.

The camera lens and aperture produce a blurred version of the object. The CCD array turns this degraded analog signal into a discrete two-dimensional (2-D) image. In addition, the images are contaminated by additive noise from various sources: quantization errors, sensor measurement, model errors, etc. Ideally, we would like to produce an HR image corresponding to placing

a high density CCD array placed *in front* of the camera lens. Although there are many different approaches (e.g., [15], [30]), we employ the following forward relationship between a degraded, LR frame and the ideal HR image [8]:

$$\mathbf{f}_k = DC_k E_k \mathbf{x} + \mathbf{n}_k, \quad 1 \leq k \leq p \quad (1)$$

$$= H_k \mathbf{x} + \mathbf{n}_k \quad (2)$$

where

- D downsampling operator;
- C_k 's blurring/averaging operators;
- E_k 's affine transforms which map the HR grid coordinate system to the LR grid systems;
- \mathbf{x} unknown ideal HR image;
- \mathbf{n}_k 's additive noise vectors.

The LR frames \mathbf{f}_k are given, and the decimation operator D is known. The blurring operator C_k and camera lens characteristics are in general unknown. However, the blurring process can be well approximated as linear spatially invariant (LSI). The scene motions for each frame relative to the reference frame are also generally not known. Finally, with multiple independent sources of error, the central limit theorem allows us to assume white Gaussian distribution for the additive noise vectors \mathbf{n}_k with possibly unknown variance. Each frame \mathbf{f}_k , $M \times N$ pixels in dimension, becomes a column $MN \times 1$ vector by columnwise reordering. Pixel (1,1) of the 2-D frame is ordered first, pixel (1,2) is second, and so forth. The unknown ideal image \mathbf{x} is reshaped into a $r^2 MN \times 1$ column by the same columnwise ordering. The matrices E_k are square $r^2 MN \times r^2 MN$ matrices representing the affine transforms applied to the ideal image. The matrices C_k , also $r^2 MN \times r^2 MN$ square matrices, represent the blurring operators, and D is an $MN \times r^2 MN$ decimation matrix. By stacking the frame equations (2) we get

$$\mathbf{f} = H\mathbf{x} + \mathbf{n} \quad (3)$$

where \mathbf{f}, \mathbf{n} are now $pMN \times 1$ vectors and H is the complete system matrix with dimensions $pMN \times r^2 MN$. The shape of the system depends on the number of available LR frames. If $p < r^2$, we have an underdetermined system. If $p = r^2$, the system will be square. And if $p > r^2$, we have an over-determined system. Techniques developed in this paper are applicable for all three cases. The matrix H is structured, typically ill-conditioned, and very large. The dimensions of H are directly related to the number of data samples and unknowns, which are usually in the tens of thousands. Even under favorable conditions where the PSF is known and noise is negligible, solving (3) is a formidable computing challenge. The reader is referred to our previous publications [24]–[26], where we have dealt with some of these computational and numerical issues.

In order to extract subpixel information content from an image sequence, each frame must be registered accurately with respect to some reference to within subpixel accuracy. In this paper, we assume that motion estimation has been performed so that image registration parameters are known explicitly. For a comprehensive review on the topic, the reader is referred to the survey by Brown [6].

III. RESTORATION AND RESOLUTION ENHANCEMENT

Image restoration and image resolution enhancement are closely related problems. In image restoration, the goal is to reconstruct the original image given a degraded (e.g., blurred) image *at the same resolution scale*. Image resolution enhancement reconstructs a higher resolution, restored image from several aliased, degraded, *low-resolution* frames. General restoration problems can be modeled as

$$\mathbf{f} = C\mathbf{x} + \mathbf{n} \quad (4)$$

where

- \mathbf{f} observed degraded image;
- \mathbf{x} original image we wish to estimate;
- \mathbf{n} various additive system noise sources;
- C convolution operator representing the blur.

In most instances, blurring is assumed to be linear shift invariant. We recover the original image \mathbf{x} by deconvolving the blur C from the degraded observed \mathbf{f} . This classical problem has been thoroughly studied and can be solved by several well-known techniques such as Wiener filtering, recursive Kalman filtering, and iterative deconvolution methods (cf. [1], [35], and [4]).

Resolution enhancement includes restoration as a special case. Namely, equation (4) can be rewritten as

$$\mathbf{f}_k = DCE_k\mathbf{x} + \mathbf{n}_k, \quad 1 \leq k \leq r^2 \quad (5)$$

where r is an arbitrary decimation factor, equivalent to the resolution enhancement factor, the LR “frames” \mathbf{f}_k ’s are the degraded data image having been shifted horizontally and vertically by multiples of one HR pixel and downsampled by a factor of r , and E_k ’s represent the relative motion shifts. Thus, image restoration can be restated as an image resolution enhancement problem with a desired enhancement factor of r and a set of r^2 LR frames with all possible horizontal and vertical HR pixel shifts to cover the entire HR grid. Fig. 3 illustrates this process, where in this example, $r = 2$. The noisy, blurred image is partitioned into four LR “frames” each marked by a distinct symbol. Using the frame marked by the circle symbol as reference, the frame marked by the square symbol contains sampling points at one HR pixel shifted in the horizontal direction. Similarly, the triangles mark sampling points at one HR pixel shifted in the vertical direction, and the diamonds sampling points at one HR pixel shifted diagonally. Image restoration is therefore simply image resolution enhancement with regularly sampled LR data completely covering the HR grid. As a result, parameter estimation techniques developed here for resolution enhancement will be applicable for restoration problems as well.

IV. BLUR IDENTIFICATION

In many practical applications, the blurring process is not known or known only to within a set of parameters. The problem of restoring the original image from a degraded observation and incomplete information about the blur is called blind deconvolution. There has been extensive work on blind deconvolution. A good survey on the topic can be found in the paper by Kundur and Hatzinakos [21]. Existing blind deconvolution methods can

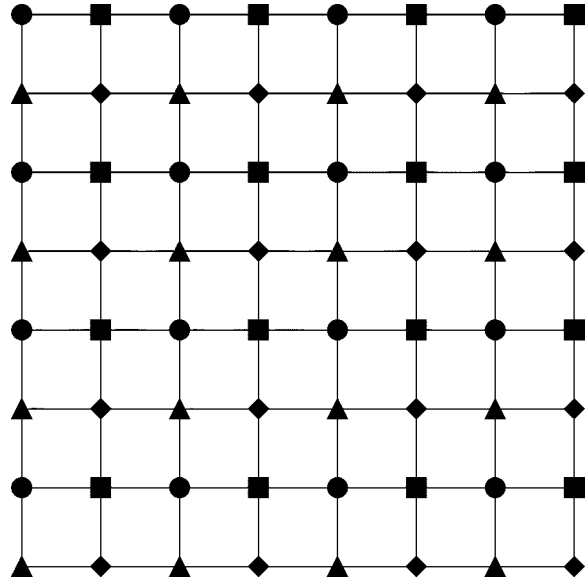


Fig. 3. Image restoration as a special case of image resolution enhancement.

be categorized into two main classes: methods which separate blur identification as a disjoint procedure from restoration, and methods which combine blur identification and restoration in one procedure. Methods in the first class tend to be computationally simpler. Blind deconvolution methods can also be generalized to handle multiple observations [31]. Multiframe blind deconvolution is better at suppressing noise and edge artifacts and preventing PSF estimates from converging to the trivial delta function.

Technically, blind deconvolution is a factorization problem of 2-D polynomials in the Z -transform domain (see e.g., [21]). Based on this observation and the fact that multidimensional polynomials are generally not factorizable, Lane and Bates [22] find the blurring and original image polynomial factors by examining the roots of the polynomial of the observed image in the Z -transform domain. Although conceptually attractive, zero sheet separation is highly sensitive to noise. Using multiple LR frames, Shekarforoush and Chellappa [32] proposed a related approach of estimating the optical transfer function (OTF) by finding spikes in the magnitude of the cross power spectrum of consecutive frames. Several researchers have considered iterative blind restoration. The most popular of these is the iterative blind deconvolution (IBD) method by Ayers and Dainty [2]. IBD simultaneously reconstructs the blur and image values by alternately enforcing constraints in the image and Fourier domain until estimates for both converge. Biggs and Andrews [5] extended the IBD method to multiple frames using the Richardson-Lucy algorithm under a maximum-likelihood (ML) framework. Similar ML approaches were proposed by Sheppard *et al.* [33], Rajagopalan and Chaudhuri [28], Harikumar and Bresler [17], and others. The simulated annealing algorithm by McCallum [23] also estimates both the blur and image values simultaneously. This method tries to find a global minimum of a cost function by randomly perturbing blur and image estimates. Kundur and Hatzinakos [21] proposed an iterative approach based on recursive inverse filtering using nonnegativity and support

constraints. They used conjugate gradient to minimize the associated cost function. In addition, several methods identify the blurring process by using special features such as edges and points, in the blurred image [27].

Other approaches [29] have simplified the identification problem by parametrizing the point spread function (PSF). With some knowledge of the imaging system and environment, we can impose a blur degradation model with a few free parameters. Blur identification is then reduced to finding best estimates for these parameters. We generalize this approach to our resolution enhancement problem. We enforce a parametric model upon the blurring process so that (1) becomes

$$\mathbf{f}_k = DC(\sigma)\mathbf{E}_k\mathbf{x} + \mathbf{n}_k, \quad 1 \leq k \leq p \quad (6)$$

$$= H_k(\sigma)\mathbf{x} + \mathbf{n}_k \quad (7)$$

where the blurring operator C is generated from a parameter set σ . The least-squares solution of (7) is the minimizer to

$$\operatorname{argmin}_{\mathbf{x}} \sum_{k=1}^p \|\mathbf{f}_k - H_k(\sigma)\mathbf{x}\|_2^2 + \lambda \mathbf{x}^T R \mathbf{x} \quad (8)$$

where λ can control the smoothness of the solution, and the stabilization (or regularization) matrix R is some symmetric positive definite matrix. For simplicity, we will consider R to be the identity matrix in this paper.² The minimizer (for the overdetermined case) to (8) can then be expressed as follows:

$$\mathbf{x}(\sigma, \lambda) = (H(\sigma)^T H(\sigma) + \lambda I)^{-1} H(\sigma)^T \mathbf{f} \quad (9)$$

$$\mathbf{f} = \begin{bmatrix} \mathbf{f}_1 \\ \vdots \\ \mathbf{f}_p \end{bmatrix}, \quad H = \begin{bmatrix} H_1 \\ \vdots \\ H_p \end{bmatrix}. \quad (10)$$

Our approach first estimates the unknown PSF parameter set σ from raw data. Once an estimate of the PSF is available, the preconditioned conjugate gradient algorithm described in a previous paper by the authors [26] is used to solve the resolution enhancement problem. In the next section, we describe our parametrized blur estimation technique using generalized cross-validation.

V. CROSS-VALIDATION

Generalized cross-validation is a popular method for computing the regularization parameter [10]. In [26], we derived the formula for GCV for underdetermined linear systems, which is typical in the resolution enhancement problem. Not surprisingly, it has the same form as in the overdetermined case.

$$\lambda_{GCV} = \operatorname{argmin}_{\lambda} \frac{\|(HH^T + \lambda I)^{-1}\mathbf{f}\|_2}{\operatorname{tr}((HH^T + \lambda I)^{-1})}. \quad (11)$$

Reeves and Mersereau have used GCV for blur identification under an autoregressive moving average (ARMA) model [29]. In a recent study by Chardon *et al.* [7], GCV has been shown to be an effective tool in parametric blur estimation. Motivated

²We note that since any positive definite choice of R can be reduced to the standard case ($R = I$) by redefining the variables, this assumption results in no loss of generality.

by these successes, we apply GCV to estimate both the PSF and regularization parameters for resolution enhancement

$$\begin{aligned} & \{\sigma_{GCV}, \lambda_{GCV}\} \\ &= \operatorname{argmin}_{\{\sigma, \lambda\}} \frac{\|(H(\sigma)H(\sigma)^T + \lambda I)^{-1}\mathbf{f}\|_2}{\operatorname{tr}((H(\sigma)H(\sigma)^T + \lambda I)^{-1})}. \end{aligned} \quad (12)$$

In [29], Reeves and Mersereau greatly simplified the minimization problem above by assuming the system matrix $H(\sigma)$ to be square and circulant, and hence, diagonalizable by the discrete Fourier transform. As a result, the numerator and denominator of the objective function in (12) could be computed easily. However, this approach is not valid for resolution enhancement because the system matrix will not typically be square or circulant. Without these assumptions, the numerator and denominator of (12) are prohibitively expensive to evaluate directly. In the later sections, we describe techniques to approximate the objective function (12) efficiently and accurately.

Reeves and Mersereau simultaneously estimated the optimal blur and regularization parameters while keeping the image model parameters fixed. We found, however, that by setting the regularization parameter to some small number, the PSF parameters can be better estimated even in the presence of noise and a small number of frames. We then use the computed PSF to determine the appropriate regularization parameter based upon the data. Our intuition is that with under-regularization, the noise effect is exacerbated and moves the GCV criterion away from possible local minima. Furthermore, the estimated PSF is less biased away from the actual PSF even though the variance of the estimates can be larger. In what follows, we first use a small value of $\lambda = \lambda_0$, so that the estimated PSF parameters can be found by solving a one-dimensional (1-D) nonlinear optimization problem

$$\sigma_{GCV} = \operatorname{argmin}_{\sigma} \frac{\|(H(\sigma)H(\sigma)^T + \lambda_0 I)^{-1}\mathbf{f}\|_2}{\operatorname{tr}((H(\sigma)H(\sigma)^T + \lambda_0 I)^{-1})}. \quad (13)$$

In the simplest case, the parameter set σ consists of one parameter describing the smoothness of the blur, e.g., the standard deviation of a Gaussian PSF or the radius of a pillbox (out-of-focus) blur. Once a blur estimate $\hat{\sigma}$ is available, we compute the regularization parameter from

$$\hat{\lambda} = \operatorname{argmin}_{\lambda} \frac{\|(H(\hat{\sigma})H(\hat{\sigma})^T + \lambda I)^{-1}\mathbf{f}\|_2}{\operatorname{tr}((H(\hat{\sigma})H(\hat{\sigma})^T + \lambda I)^{-1})}. \quad (14)$$

VI. QUADRATURE RULES WITH LANCZOS ALGORITHM

For large systems, numerators and denominators in (13) and (14) are very expensive to evaluate directly. We first approximate the denominator using an unbiased trace estimator introduced by Hutchinson [19]: Let U be a discrete random variable which takes the values -1 and $+1$ each with probability $1/2$, and let \mathbf{u} be a vector whose entries are independent samples from U . Then the term $\mathbf{u}^T(HH^T + \lambda I)^{-1}\mathbf{u}$ is an unbiased estimator of $\operatorname{tr}((HH^T + \lambda I)^{-1})$.

Now, in order to estimate both the numerators and denominators in (13) and (14), we need to estimate quadratic forms $\mathbf{v}^T f(M) \mathbf{v}$, where M is some symmetric positive definite matrix and $f(\xi) = \xi^{-p}$, $p = 1, 2$. There is extensive literature

on the application of Gauss quadrature rules to bound bilinear forms; see papers by Golub and collaborators [3], [9], [11], [12], [14]. This paper applies these techniques to our blur identification problem.

Let the eigendecomposition of M be given by $M = Q^T \Xi Q$, where Q is an orthogonal matrix and Ξ is a diagonal matrix of eigenvalues in increasing order. Then

$$\begin{aligned} \mathbf{v}^T f(M) \mathbf{v} &= \mathbf{v}^T Q^T f(\Xi) Q \mathbf{v} \\ &= \tilde{\mathbf{v}}^T f(\Xi) \tilde{\mathbf{v}} \\ &= \sum_{i=1}^n f(\xi_i) \tilde{v}_i^2 \end{aligned} \quad (15)$$

where $\tilde{\mathbf{v}} = (\tilde{v}_i) \equiv Q\mathbf{v}$. Suppose that we have bounds on the spectrum of M , (e.g., by Gershgorin circle theorem), such that $a \leq \xi_1 \leq \dots \leq \xi_n \leq b$. The last sum can be considered as a Riemann–Stieltjes integral with nondecreasing piecewise constant measure [14]

$$\sum_{i=1}^n f(\xi_i) \tilde{v}_i^2 = \int_a^b f(\xi) d\mu(\xi) \quad (16)$$

where the measure $\mu(\xi)$ is defined as

$$\mu(\xi) = \begin{cases} 0, & \text{if } \xi < \xi_1 \\ \sum_{j=1}^i \tilde{v}_j^2, & \text{if } \xi_i \leq \xi < \xi_{i+1} \\ \sum_{j=1}^n \tilde{v}_j^2, & \text{if } \xi_n \leq \xi. \end{cases} \quad (17)$$

The key to efficiently and accurately estimating the quadratic forms is that we can approximate the Riemann–Stieltjes integral (16) with Gauss-type quadrature rules.

The general form for quadrature rules is

$$\begin{aligned} I[f] &= \sum_{i=1}^k \omega_i f(\theta_i) + \sum_{j=1}^l \nu_j f(\tau_j), \\ \int_a^b f(\xi) d\mu(\xi) &= I[f] + R[f] \end{aligned} \quad (18)$$

where the weights ω_i and ν_j and the nodes θ_i are unknown, the nodes τ_j are predetermined, and $R[f]$ is the error term. The Gauss-type quadrature rules differ from one another by the number of prescribed nodes. If there are no prescribed nodes, then we obtain the standard Gauss quadrature:

$$I_G[f] = \sum_{i=1}^k \omega_i f(\theta_i). \quad (19)$$

If one node is prescribed, we get the Gauss–Radau quadrature rule; with two nodes prescribed, the Gauss–Lobatto rule

$$I_R[f] = \sum_{i=1}^k \omega_i f(\theta_i) + \nu f(\tau) \quad (20)$$

$$I_L[f] = \sum_{i=1}^k \omega_i f(\theta_i) + \nu_1 f(\tau_1) + \nu_2 f(\tau_2). \quad (21)$$

The Gauss–Radau rule is often applied with either $\tau = a$ or $\tau = b$. Gauss–Lobatto has both endpoints prescribed, $\tau_1 = a, \tau_2 = b$. As will be described below, we can compute the unknown nodes θ_i and weights ω_i, ν_i for these Gauss-type rules

TABLE I
MSE IN PSF ESTIMATES FOR GAUSSIAN BLUR WITH 10 RANDOMLY CHOSEN FRAMES—EXAMPLE I

σ	SNR		
	∞ dB	60 dB	30 dB
0.75	3.43	3.27	4.79
1.00	0.02	0.02	0.53
2.00	0.01	0.01	0.11

TABLE II
MSE IN PSF ESTIMATES FOR GAUSSIAN BLUR WITH ALL 16 FRAMES AVAILABLE—EXAMPLE I

σ	SNR		
	∞ dB	60 dB	30 dB
0.75	0.00	0.00	3.93
1.00	0.04	0.04	0.17
2.00	0.00	0.00	0.09

from recurrence coefficients of sequences of orthogonal polynomials via the Lanczos bidiagonalization algorithm (cf. [11] and [14]). The next subsection describes quadrature bounds on quadratic forms.

A. Quadrature Error and Bounds

The quadrature error $R[f]$ from (18) can be expressed as

$$R[f] = \frac{f^{(2k+l)}(\eta)}{(2k+l)!} \int_a^b \prod_{j=1}^l (\xi - \tau_j) \prod_{i=1}^k (\xi - \theta_i)^2 d\mu(\xi) \quad (22)$$

for some $\eta \in (a, b)$. We have the following bound for the Gauss quadrature rule [11].

Theorem 1: Suppose that $f^{(2k)}(\xi) > 0, \forall k, \forall \xi, a < \xi < b$, then

$$I_G[f] \leq \int_a^b f(\xi) d\mu(\xi). \quad (23)$$

Proof: For the Gauss rule, there are no prescribed nodes, so

$$R_G[f] = \frac{f^{(2k)}(\eta)}{(2k)!} \int_a^b \prod_{i=1}^k (\xi - \theta_i)^2 d\mu(\xi). \quad (24)$$

Since $f^{(2k)}(\eta) > 0, \forall k, \forall \eta, a < \eta < b$, and $\int_a^b \prod_{i=1}^k (\xi - \theta_i)^2 d\mu(\xi) \geq 0$, then $R_G[f] \geq 0$. Therefore

$$I_G[f] \leq \int_a^b f(\xi) d\mu(\xi). \quad (25)$$

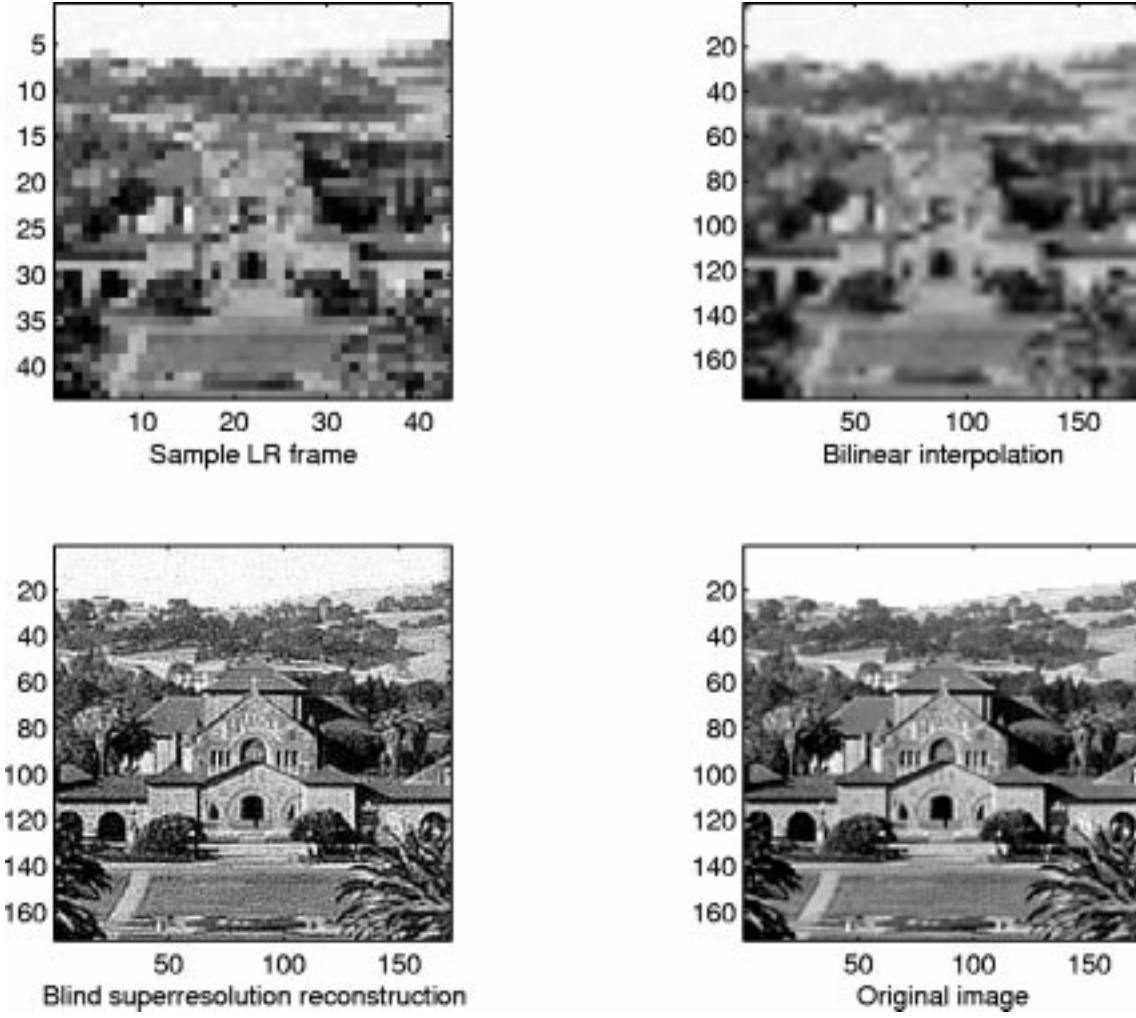


Fig. 4. Parametric resolution enhancement for synthetic sequence—example I, 30 dB.

Analogous theorems for Gauss–Radau and Gauss–Lobatto rules are also available. \square

Theorem 2: Suppose that $f^{(2k+1)}(\xi) < 0, \forall k, \forall \xi, a < \xi < b$, then

$$I_{Rb}[f] \leq \int_a^b f(\xi) d\mu(\xi) \leq I_{Ra}[f] \quad (26)$$

where $I_{Ra}(I_{Rb})$ corresponds to Gauss–Radau rule with prescribed node at $\tau = a(b)$. \square

Proof: Similar proof as in Theorem 1. \square

Theorem 3: Suppose that $f^{(2k)}(\xi) > 0, \forall k, \forall \xi, a < \xi < b$, then

$$\int_a^b f(\xi) d\mu(\xi) \leq I_L[f] \quad (27)$$

with prescribed nodes $\tau_1 = a, \tau_2 = b$. \square

Proof: Similar proof as in Theorem 1. \square

Recall that the quadratic terms which we are interested in approximating have form $\mathbf{v}^T M^{-p} \mathbf{v}, p = 1, 2$. The function $f(\xi) = \xi^{-p}$ satisfies the hypotheses of Theorems 1, 2, and 3, for M positive definite ($a > 0$). Hence, we can apply the above

theorems to bound $\int_a^b f(\xi) d\mu(\xi)$ with Gauss-type quadrature rules. Define

$$L[f] := \max(I_G[f], I_{Rb}[f]) \quad (28)$$

$$U[f] := \min(I_{Ra}[f], I_L[f]) \quad (29)$$

where $I_{Ra}(I_{Rb})$ is the Gauss–Radau rule with the prescribed node at $\tau = a(b)$. We have the following bounds

$$L[f] \leq \int_a^b f(\xi) d\mu(\xi) \leq U[f]. \quad (30)$$

As the number of nodes k increases, the bounds $L[f]$ and $U[f]$ become tighter. To find quadrature bounds $L[f]$ and $U[f]$, we need the unknown weights and nodes ω_i, ν_j , and θ_i . Appendix A describes how these quantities can be computed from sequences of orthogonal polynomials associated with the weight measure $d\mu(\xi)$. In practice, we use $U[f]$ as the approximate value for $\int_a^b f(\xi) d\mu(\xi) := \mathbf{v}^T f(M) \mathbf{v}$.

VII. EXPERIMENTS

We estimate blur and regularization parameters using the GCV criterion with quadrature rule bounds as described above.

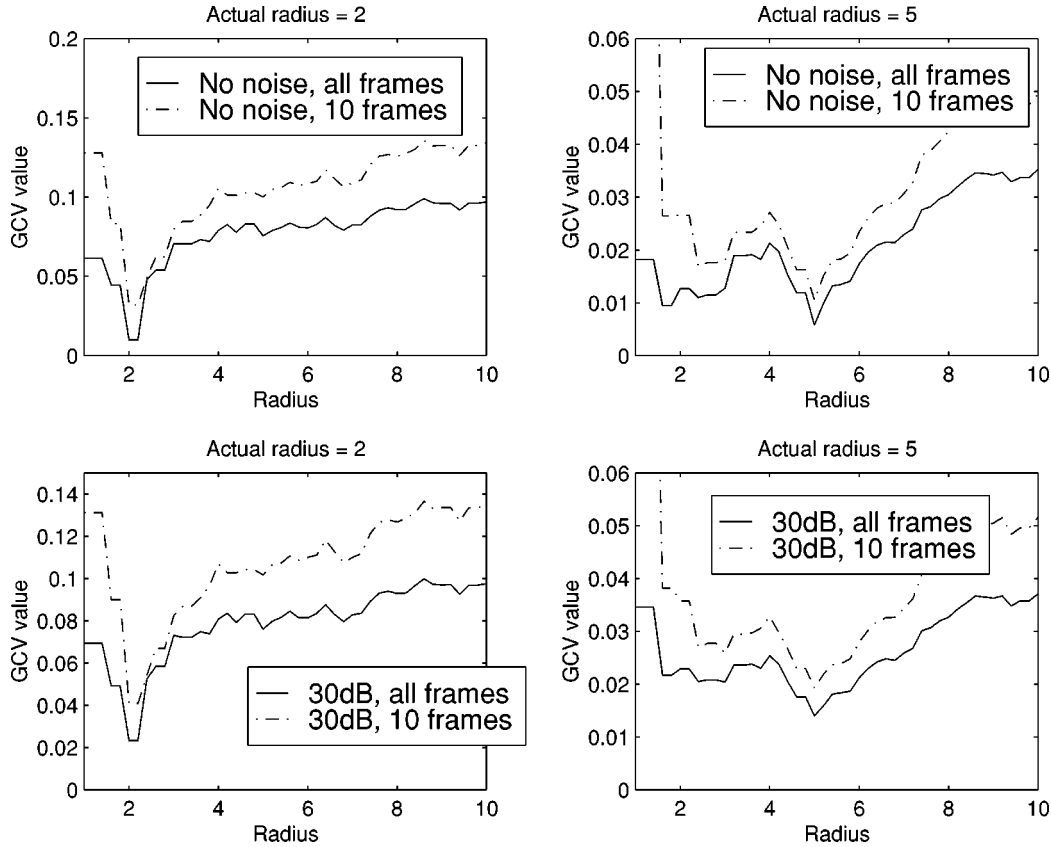


Fig. 5. GCV plot for pillbox blur—example I.

In our experiments, we assume simple PSF models with one unknown blur parameter, designed to illustrate our methods. In most realistic blur identification applications, these models can be used as initial estimates.

We use Matlab's CONSTR routine [20] to solve the GCV minimization problem (13). For each function evaluation however, we iterate with the Lanczos algorithm with the following stopping criterion:

$$\frac{U[f] - L[f]}{U[f]} \leq 0.01.$$

For our test image sequences, Lanczos usually terminates within 70 iterations, equivalent to 140 matrix-vector multiplies. The iteration count is quite low compared to the dimensions of the system matrix (usually in the tens of thousands).

Example I: In the first set of experiments, 16 LR frames are generated by blurring a 172×172 pixel HR image of the Stanford quad, with a 4×4 Gaussian blur and downsampling by a factor of four in each dimension. We experiment with blurs of standard deviations 0.75, 1, and 2 and try to estimate these parameters assuming the support of the PSF to be known. We use the nonlinear PSF parameter estimation (13) with $\lambda_0 = 0.001$. In addition, we consider realizations of 60 dB, 30 dB SNR³ and without additive Gaussian noise added to the LR frames. Tables I and II display the mean square error (MSE) of the PSF estimates under these conditions, with ten randomly chosen LR

³Signal to noise ratio (SNR) is defined as $10 \log_{10} \frac{\sigma^2}{\sigma_n^2}$, where σ^2, σ_n^2 are variances of a clean frame and noise, respectively.

frames and with all 16 frames, respectively. The formula for calculating percent MSE is [7]

$$\text{MSE}(\hat{\sigma}) = 100 \frac{\|ch(\hat{\sigma}) - h(\sigma)\|_2^2}{\|h(\sigma)\|_2^2}$$

where $h(\hat{\sigma})$ is the PSF estimate of $h(\sigma)$, and the scaling factor

$$c = \frac{h(\hat{\sigma}) \cdot h(\sigma)}{\|h(\hat{\sigma})\|_2^2}.$$

These tables show excellent PSF reconstruction results for all cases. Next, in Fig. 4, we quantitatively compare the parametric resolution enhancement reconstruction result against the original HR image. The actual blur standard deviation in this example is 0.75. We add white noise to the ten LR frames to realize an SNR of 30 dB. We compute first the PSF estimate from (13) using $\lambda_0 = 0.001$ as above. With this estimated PSF, we obtain a regularization parameter by solving (14), which is found to be 0.0249. Fig. 4 shows the result of resolution enhancement using computed PSF and regularization parameters.

In the second set of experiments, we run tests for a pillbox (defocussed) blur. The parameter to be estimated is the radius of the blur. Our experiments test for out-of-focus blurs with radii 2 and 5 using the LR Stanford frames. We plot GCV values for radius taking values from 1 to 10 at 0.2 intervals in Fig. 5. The plots show that GCV function achieves global minimum at the correct values in all cases.

Example II: The LR FLIR images in our final parametric resolution enhancement experiment are provided courtesy of

Brian Yasuda and the FLIR research group in the Sensors Technology Branch, Wright Laboratory, WPAFB, OH. Each image is 64×64 pixels and a resolution enhancement factor of five is sought after. The objects in the scene are stationary, and 16 frames are acquired by controlled movements of a FLIR imager described in [16]. The frame to frame motions are accurately known for this sequence. We first estimate the blur variance assuming a Gaussian blur with support equaling the resolution enhancement factor, using (13) with $\lambda_0 = 0.001$. Similar to the process outlined in example I, we compute the regularization parameter using the PSF estimate, which turns out to be 0.0174. Fig. 6 shows a sample LR frame from the FLIR sequence and the resulting HR image using the computed variance and regularization parameter.

VIII. CONCLUSION

We propose a parametric blur and regularization estimation approach, based on the generalized cross-validation method, for restoration/resolution enhancement. We solve a multivariate nonlinear minimization problem for these unknown parameters. To efficiently and accurately estimate the numerator and denominator of the GCV objective function, we present Gauss-type quadrature techniques for bounding quadratic forms. Experimental results from a synthetic image sequence show that blur parameters are accurately approximated from Gaussian and pillbox blurs under various conditions. Image resolution enhancement results using these computed values are visually pleasing as well. Successful experiments with a real FLIR image sequence illustrate that our techniques can be a foundation for data-driven efficient restoration/resolution enhancement algorithms.

APPENDIX A

ORTHOGONAL POLYNOMIALS AND THE LANCZOS ALGORITHM

Recall from Section VI that we bound quadratic form $\mathbf{v}^T f(M)\mathbf{v}$, where M is symmetric positive definite, with Gauss-type quadrature rules of the form

$$I[f] = \sum_{i=1}^k \omega_i f(\theta_i) + \sum_{j=1}^l \nu_j f(\tau_j).$$

As mentioned previously, the unknown nodes θ_i and weights ω_i, ν_i needed to calculate these quadrature values are related to the roots of orthogonal polynomials associated with the weight measure $d\mu(\xi)$ and the coefficients of their three-term recurrence. The following subsection describes orthogonal polynomials in more detail and outlines the Lanczos bidiagonalization used to efficiently compute the recurrence coefficients and quadrature values.

A. Orthogonal Polynomials

For a nondecreasing piecewise constant weight function $\mu(\xi)$, we can define a sequence of orthonormal polynomials $\{p_i\}_{i=0}^{n-1}$ such that

$$\int_a^b p_i(\xi) p_j(\xi) d\mu(\xi) = \begin{cases} 1, & \text{if } i = j, \\ 0, & \text{if } i \neq j. \end{cases} \quad (31)$$

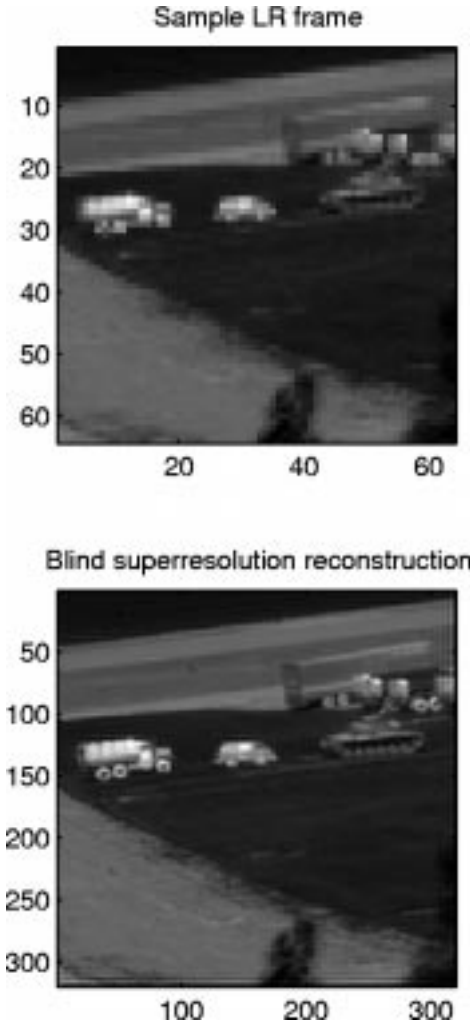


Fig. 6. Parametric resolution enhancement for FLIR sequence—example II.

These polynomials satisfy a three-term recurrence relation (see [34])

$$\xi \mathbf{p}_k(\xi) = T_k \mathbf{p}_k(\xi) + \beta_k p_k(\xi) \mathbf{e}_k, \quad k = 1, \dots, n, \quad (32)$$

$$p_{-1}(\xi) = 0, \quad p_0(\xi) = 1 \quad (33)$$

with

$$\mathbf{e}_k = \begin{bmatrix} 0 \\ \vdots \\ 0 \\ 1 \end{bmatrix}, \quad \mathbf{p}_k = \begin{bmatrix} p_0(\xi) \\ \vdots \\ p_{k-1}(\xi) \end{bmatrix}$$

$$T_k = \begin{bmatrix} \alpha_1 & \beta_1 & & & \\ \beta_1 & \ddots & \ddots & & \\ & \ddots & \ddots & \ddots & \\ & & \alpha_{k-1} & \beta_{k-1} & \\ & & \beta_{k-1} & \alpha_k & \end{bmatrix}. \quad (34)$$

It can be shown that the nodes θ_i of Gauss quadrature rule are the eigenvalues of T_k , which are also the zeros of the polynomial p_n . The weights ω_i are the square of the first component of the normalized eigenvectors of T_k . The Gauss quadrature approximation is given by (see [13])

$$I_G[f] = \|\mathbf{v}\|^2 \mathbf{u}_1^T f(T_k + \lambda I) \mathbf{u}_1 \quad (35)$$

TABLE III
LANCZOS BIDIAGONALIZATION ALGORITHM

$\mathbf{q}_0 = \mathbf{b}/\ \mathbf{b}\ _2$
$\mathbf{s}_0 = A^T \mathbf{q}_0$
$\gamma_1 = \ \mathbf{s}_0\ _2$
$\mathbf{w}_0 = \mathbf{s}_0/\gamma_1$
for $k = 2 : n$ do
$\mathbf{r}_{k-1} = A\mathbf{w}_{k-2} - \gamma_{k-1}\mathbf{q}_{k-2}$
$\delta_{k-1} = \ \mathbf{r}_{k-1}\ _2$
$\mathbf{q}_{k-1} = \mathbf{r}_{k-1}/\delta_{k-1}$
$\mathbf{s}_{k-1} = A^T \mathbf{q}_{k-1} - \delta_{k-1}\mathbf{w}_{k-2}$
$\gamma_k = \ \mathbf{s}_{k-1}\ _2$
$\mathbf{w}_{k-1} = \mathbf{s}_{k-1}/\gamma_k$
end

where $\mathbf{u} = [1 \ 0 \ \dots \ 0]^T$ is a k -vector with one in the first entry and zeros elsewhere. For the Gauss–Radau rule, we need to adjust the last entry α_k of T_k so that the adjusted tridiagonal matrix \hat{T}_k has an eigenvalue at the prescribed node [9], [3]. For the Gauss–Lobatto rule, the last three nonzero entries $\beta_{k-1}, \alpha_k, \beta_{k-1}$ will be adjusted to prescribe eigenvalues at a and b .

Following [3], for the Gauss–Radau rule, in order to prescribe a node at either a or b , we replace the last entry α_k of T_k by

$$\phi = \tau + s_{k-1} \quad (36)$$

with $\tau = \{a, b\}$ and s_{k-1} being the last component of the solution \mathbf{s} to

$$(T_{k-1} - \tau I)\mathbf{s} = \beta_{k-1}^2 \mathbf{e}_{k-1}, \quad (37)$$

$$\beta_{k-1} = (\gamma_{k-1} + \gamma_k)\delta_{k-1}. \quad (38)$$

For Gauss–Lobatto rule, to prescribe nodes at a and b , the last three nonzero entries $\beta_{k-1}, \alpha_k, \beta_{k-1}$ are replaced by ψ, ϕ, ψ , where

$$\phi = \frac{s_{k-1}b - t_{k-1}a}{s_{k-1} - t_{k-1}}, \quad \psi^2 = \frac{b - a}{s_{k-1} - t_{k-1}} \quad (39)$$

where s_{k-1} and t_{k-1} are the last components of the solutions \mathbf{s} and \mathbf{t} to

$$(T_{k-1} - aI)\mathbf{s} = \mathbf{e}_{k-1} \quad (T_{k-1} - bI)\mathbf{t} = \mathbf{e}_{k-1}. \quad (40)$$

For Gauss–Radau and Gauss–Lobatto rules, the quadrature approximations have the form

$$I[f] = \|\mathbf{v}\|^2 \mathbf{u}_1^T f(\tilde{T}_k + \lambda I) \mathbf{u}_1 \quad (41)$$

where \tilde{T}_k is the tridiagonal matrix T_k with the last few entries adjusted accordingly.

The entries of T_k can be computed via the Lanczos bidiagonalization algorithm as follows.

B. Lanczos Bidiagonalization

The matrix T_k is the tridiagonal matrix resulting from k iterations of Lanczos bidiagonalization algorithm for M with $\mathbf{v}/\|\mathbf{v}\|_2$ as the starting vector. In Table III, we include the Lanczos bidiagonalization factorization algorithm to efficiently compute the entries of T_k . After k iterations of the Lanczos bidiagonalization algorithm, we obtain an orthogonal $m \times k$ matrix

$$Q_k = [\mathbf{q}_0 \cdots \mathbf{q}_{k-1}] \quad (42)$$

and an $n \times k$ orthogonal matrix

$$W_k = [\mathbf{w}_0 \cdots \mathbf{w}_{k-1}] \quad (43)$$

with the following relations:

$$AW_k = Q_k B_k + \delta_k \mathbf{q}_k \mathbf{e}_k^T, \quad (44)$$

$$A^T Q_k = W_k B_k^T \quad (45)$$

where B_k is a $k \times k$ lower bidiagonal matrix

$$B_k = \begin{bmatrix} \gamma_1 & & & \\ \delta_1 & \ddots & & \\ & \ddots & \ddots & \\ & & \delta_{k-1} & \gamma_k \end{bmatrix}. \quad (46)$$

Combining (44) and (45), we get

$$AA^T Q_k = Q_k B_k B_k^T + \gamma_k \delta_k \mathbf{q}_k \mathbf{e}_k^T. \quad (47)$$

The tridiagonal T_k in (32) is exactly $B_k B_k^T$.

REFERENCES

- [1] H. Andrews and B. Hunt, *Digital Image Restoration*. Englewood Cliffs, NJ: Prentice-Hall, 1977.
- [2] G. Ayers and J. Dainty, “Iterative blind deconvolution method and its applications,” *Opt. Lett.*, vol. 13, no. 7, 1988.
- [3] Z. Bai, M. Fahey, and G. Golub, “Some large-scale matrix computation problems,” *J. Comput. Appl. Math.*, vol. 74, pp. 71–89, 1996.
- [4] J. Biemond, R. Lagendijk, and R. Mersereau, “Iterative methods for image deblurring,” *Proc. IEEE*, vol. 78, pp. 856–883, May 1990.
- [5] D. Biggs and M. Andrews, “Asymmetric iterative blind deconvolution of multiframe images,” in *Proc. SPIE Conf. Advanced Signal Processing Algorithms, Architectures, Implementations VII*, San Diego, CA, July 1998.
- [6] L. Brown, “A survey of image registration techniques,” *ACM Comput. Surv.*, vol. 24, no. 4, pp. 325–376, Dec. 1992.
- [7] S. Chardon, B. Vozel, and K. Chehdi, “A comparative study between parametric blur estimation methods,” in *Proc. Int. Conf. Acoustic, Speech, Signal Processing '99*, Phoenix, AZ, 1999.
- [8] M. Elad, “Super-resolution reconstruction of images,” Ph.D. dissertation, The Technion—Israel Inst. Technol., Haifa, Dec. 1996.
- [9] G. Golub, “Some modified matrix eigenvalue problem,” *SIAM Rev.*, vol. 15, pp. 318–334, 1973.
- [10] G. Golub, M. Heath, and G. Wahba, “Generalized cross-validation as a method for choosing a good ridge parameter,” *Technometrics*, vol. 21, pp. 215–223, 1979.
- [11] G. Golub and G. Meurant, “Matrices, moments, and quadrature,” in *Numerical Analysis 1993*, D. F. Griffiths and G. A. Watson, Eds., Longman, Essex, U.K., 1994, pp. 105–156.
- [12] G. Golub and Z. Strakos, “Estimates in quadratic formulas,” *Numer. Algor.*, vol. 8, pp. 241–268, 1994.
- [13] G. Golub and U. von Matt, “Generalized cross-validation for large-scale problems,” *J. Comput. Graph. Statist.*, vol. 6, pp. 1–34, 1997.
- [14] G. Golub and J. Welsch, “Calculation of Gauss quadrature rules,” *Math. Comput.*, vol. 23, pp. 221–230, 1969.

- [15] D. Granrath and J. Lersch, "Fusion of images on affine sampling grids," *JOSA-A*, vol. 15, no. 4, pp. 791–801, 1998.
- [16] R. Hardie, K. Barnard, and E. Armstrong, "Joint MAP registration and high-resolution image estimation using a sequence of undersampled images," *IEEE Trans. Image Processing*, vol. 6, pp. 1621–1633, Dec. 1997.
- [17] G. Harikumar and Y. Bresler, "Perfect blind restoration of images blurred by multiple filters: Theory and efficient algorithms," *IEEE Trans. Image Processing*, vol. 8, pp. 202–219, Feb. 1999.
- [18] B. Hunt, "Super-resolution of images: Algorithms, principles, and performance," *Int. J. Imag. Syst. Technol.*, vol. 6, no. 4, pp. 297–304, 1995.
- [19] M. Hutchinson, "A stochastic estimator of the trace of the influence matrix for laplacian smoothing splines," *Commun. Statist., Simul., Comput.*, vol. 19, pp. 433–450, 1990.
- [20] *MATLAB, High-Performance Numeric Computation and Visualization Software*, 1992.
- [21] D. Kundur and D. Hatzinakos, "Blind image deconvolution," *IEEE Signal Processing Mag.*, vol. 13, pp. 43–64, May 1996.
- [22] R. Lane and R. Bates, "Automatic multidimensional deconvolution," *J. Opt. Soc. Amer. A*, vol. 4, no. 1, pp. 180–188, Jan. 1987.
- [23] B. McCallum, "Blind deconvolution by simulated annealing," *Opt. Commun.*, vol. 75, no. 2, pp. 101–105, Feb. 1983.
- [24] N. Nguyen, "Numerical techniques for image superresolution," Ph.D. dissertation, Stanford Univ., Stanford, CA, Apr. 2000.
- [25] N. Nguyen and P. Milanfar, "A fast wavelet interpolation-restoration method for superresolution," *Circuits, Syst., Signal Process.*, vol. 19, no. 4, 2000.
- [26] N. Nguyen, P. Milanfar, and G. Golub, "A computationally efficient superresolution image reconstruction algorithm," *IEEE Trans. Image Processing*, vol. 10, pp. 573–583, Apr. 2001.
- [27] K. Nishi and S. Ando, "Blind superresolving image recovery from blur-invariant edges," in *Proc. of Int. Conf. Acoustics, Speech, Signal Processing '94*, vol. 5, 1994, pp. 85–88.
- [28] A. Rajagopalan and S. Chaudhuri, "A recursive algorithm for maximum likelihood-based identification of blur from multiple observations," *IEEE Trans. Image Processing*, vol. 7, pp. 1075–1079, July 1998.
- [29] S. Reeves and R. Mersereau, "Blur identification by the method of generalized cross-validation," *IEEE Trans. Image Processing*, vol. 1, pp. 301–311, July 1992.
- [30] R. Schultz and R. Stevenson, "Extraction of high-resolution frames from video sequences," *IEEE Trans. Image Processing*, vol. 5, pp. 996–1011, June 1996.
- [31] T. Schulz, "Multiframe blind deconvolution of astronomical images," *JOSA-A*, vol. 10, no. 5, pp. 1064–1073, 1993.
- [32] H. Shekarforoush and R. Chellappa, "Data-driven multi-channel superresolution with application to video sequences," *J. Opt. Soc. Amer. A*, vol. 16, no. 3, pp. 481–492, Mar. 1999.
- [33] D. Sheppard, B. Hunt, and M. Marcellin, "Iterative multiframe super-resolution algorithms for atmospheric-turbulence-degraded imagery," *J. Opt. Soc. Amer. A*, vol. 15, no. 4, pp. 978–992, Apr. 1998.
- [34] G. Szegő, *Orthogonal Polynomials*, 3rd ed. Memphis, TN: Amer. Math. Soc., 1974.
- [35] J. Woods and V. Ingle, "Kalman filtering in two dimensions: Further results," *IEEE Trans. Acoust., Speech, Signal Processing*, vol. ASSP-29, pp. 188–197, Apr. 1981.



Nhat Nguyen received B.S. degrees in mathematics and computer science from the California Institute of Technology, Pasadena, in 1994, and the Ph.D. degree from the Scientific Computing and Computational Mathematics Program, Stanford University, Stanford, CA, in 2000.

He is currently a Software Engineer with the Surf-scan Division of KLA-Tencor Corporation, San Jose, CA. His technical interests are in signal and image processing algorithms and numerical linear algebra.



Peyman Milanfar (S'89–M'93–SM'98) received the B.S. degree in engineering mathematics from the University of California, Berkeley, in 1988, and the S.M., E.E., and Ph.D. degrees in electrical engineering from the Massachusetts Institute of Technology, Cambridge, in 1990, 1992, and 1993, respectively.

From 1993 to 1994, he was a Member of Technical Staff at Alphatech, Inc., Burlington, MA. From 1994 to 1999, he was a Senior Research Engineer at SRI International, Menlo Park, CA. He is currently an Assistant Professor of electrical engineering at the University of California, Santa Cruz. He was a Consulting Assistant Professor of computer science at Stanford University, Stanford, CA, from 1998 to 2000. His technical interests are in statistical and numerical methods for signal and image processing, and, more generally, inverse problems, particularly those involving moments.

Dr. Milanfar was awarded a National Science Foundation CAREER Grant in January 2000. He is an associate editor for the IEEE SIGNAL PROCESSING LETTERS.



Gene Golub was born in Chicago, IL, in 1932. He received the Ph.D. degree from the University of Illinois, Urbana, in 1959.

He held an NSF Fellowship at the University of Cambridge, Cambridge, U.K. He joined the faculty of Stanford University, Stanford, CA, in 1962, where he is currently the Fletcher Jones Professor of Computer Science and the Director of the Program in Scientific Computing and Computational Mathematics. He served as Chairman of the Computer Science Department from 1981 until 1984. He is noted for his work in the use of numerical methods in linear algebra for solving scientific and engineering problems. This work resulted in a book *Matrix Computations* (Baltimore, MD: Johns Hopkins University Press, 1996) co-authored with Charles Van Loan. He has served as President of the Society of Industrial and Applied Mathematics (1985–1987) and is the Founding Editor of the *SIAM Journal of Scientific and Statistical Computing* and the *SIAM Journal of Matrix Analysis and Applications*. He is the originator of na-net.

Dr. Golub holds several honorary degrees. He is a member of the National Academy of Engineering, the National Academy of Sciences, and the American Academy of Sciences.